Accepted Manuscript

Bending response of carbon fiber composite sandwich beams with three dimensional honeycomb cores

Jian Xiong, Li Ma, Ariel Stocchi, Jinshui Yang, Linzhi Wu, Shidong Pan

PII: S0263-8223(13)00482-0
DOI: http://dx.doi.org/10.1016/j.compstruct.2013.09.035
Reference: COST 5367

To appear in: *Composite Structures*

Bending response of carbon fiber composite sandwich beams with three dimensional honeycomb cores

Jian Xiong [a*], Li Ma [a], Ariel Stocchi [b], Jinshui Yang [a], Linzhi Wu [a], Shidong Pan [a*]
[a] Center for Composite Materials and Structures, Harbin Institute of Technology
Harbin 150001, China
[b] Research Institute of Material Science and Technology (INTEMA) - National University of Mar del Plata (UNMdP), Mar del Plata, Argentina

Abstract:

Bending properties and failure modes of carbon fiber composite Egg and pyramidal honeycomb beams were studied and presented in this paper. Three point bending responses of both sandwich beams were tested. Face wrinkling, face crushing, core member crushing and debonding were considered, and theoretical relationships for predicting the failure load associated with each mode were presented under three point bending load. Failure mechanism maps were constructed to predict the failure of composite sandwich beams with pyramidal and egg honeycomb cores subjected to bending. Face wrinkling and core debonding have been investigated under three point bending and the maximum displacement was studied using analytical and experimental methods. The finite element method was employed to determine the ratio (maximum displacement/applied load) of sandwich beam with two different honeycomb cores. Comparisons between two kinds of honeycomb beams were also conducted.

Keywords: Sandwich beam; Honeycomb; Bending; Mechanical properties; Analytical modeling.

[*] Corresponding author, Tel.:+86 451 86402376; fax: +86 451 86402376.
E-mail address: jx@hit.edu.cn (Jian Xiong) sd6419866@sina.com (Shidong Pan)

1. Introduction

Sandwich structures effectively provide lightweight stiffness and strength by sandwiching a low-density core between stiff face sheets. The core materials were traditionally manufactured using stochastic metal or polymer foams [1-3], corrugated [4] honeycomb [5-6] and truss materials [7-8]. These combinations of properties are very important in the development of many contemporary vehicles and structures. Usage of fiber-reinforced composites in sandwich structures generally allows an additional weight reduction without jeopardizing the strength and performance of the structure. Thus, sandwich panels made of fiber-reinforced composites are attractive for building ultra-light, high-strength components, specifically for the aerospace industry and flight structures [9]. The behavior of flax and nature fiber composite honeycomb cores were investigated under low velocity impact loading by Petrone et al [10-11]. Han and Tsai [12] introduced interlocked grid structures with pultruded glass fiber ribs. The interlocking method has been mainly used to manufacture square honeycomb at lower cost compared to hot press [13] and laser cutting methods [14]. Larger-sized, mass-produced sandwich panels have many potential applications in building large-scale structures and ships. In addition, they are energy absorbent [15-16] and attenuate sound transmission [17-18] and heat transfer [19]. Three dimensional honeycomb cores were developed for combining load-bearing structures with multifunctional benefits. The hollow cores with interconnected void spaces can be used to embed electronics and foam to carry out multifunctional applications.

Bending property is very important in the design of lightweight sandwich beams.

There is much literature available pertaining to the bending behavior of sandwich beams with various kinds of cores. Liu et al. [20] presented a semi-analytical method for the bending analysis of sandwich panels with square honeycomb cores. He et al. [21] then demonstrated that the stiffness performance of the corrugated core, honeycomb core and X-core sandwich panels with the same structural weight are very close, with that of the honeycomb core sandwich panel a little better than the other sandwich panels. Rathbun et al. [22] have investigated the bending behavior of lightweight metallic sandwich structures with tetrahedral truss cores. Zok et al [23] reported a protocol for characterizing the bending performance of metal sandwich panels with pyramidal truss cores. Valdevit et al [24] presented the optimized results regarding sandwich panels with prismatic cores under bending load. Jin et al. [25] conducted bending tests in order to reveal the mechanical property and the failure mechanism of integrated woven corrugated sandwich composites. Liu et al [26-27] have performed analytical modeling and simulation of the structural performance of sandwich beams with pin-reinforced foam cores and truss cores under bending. Russell et al [28] manufactured carbon fiber composite square honeycombs that are mainly used as load bearing structures, and the multifunctional benefit is very limited; the bending behavior was then studied using analytical predictions, measurements and finite element simulations [29]. Li et al. [30] studied the bending behavior of three-dimensional pyramidal truss sandwich beams, and the failure mechanisms were investigated. The interlocked cores reinforced by carbon fibers of the Kagome grid were manufactured and tested by Fan et al [31]; the bending properties of Kagome and improved carbon fiber reinforced lattice-core sandwich beams were then investigated [32]. In our previous work [33-34], the out-of-plane and in-plane compressive properties of carbon fiber composite sandwich panels with three-dimensional honeycomb cores were studied. To date, however, there is no research work on the bending behaviors of sandwich beams with three-dimensional honeycomb cores since this innovative core architecture appeared recently for designing lightweight and multifunctional sandwich structures. The fabricated carbon fiber composite three-dimensional honeycomb cores and sandwich panels are shown in Figure 1 and 2 for egg and pyramidal honeycomb cores, respectively. The properties of the parent material (T700/epoxy composite) are listed in Table 1. In the present paper, the bending properties and failure mechanism of carbon fiber composite sandwich beams with egg or pyramidal honeycomb cores have been researched using analytical predictions, experimental tests and simulations. The details of the analytical predictions for the egg and pyramidal honeycomb beams under three point bending are derived in section 2. In section 3, the experiments were conducted to study the bending behavior of the three-dimensional honeycomb beams and compared to analytical results. In section 4, the finite element models have been built in order to predict the bending behavior of sandwich beams. At last, the conclusions are drawn in section 5.

2. Experimental

2.1 Fabrication

A method for fabricating carbon fiber composite egg and pyramidal honeycomb cores has been developed in our previous paper [33]. In this work, the plate interlocking method has been used to form the core. First, carbon fiber composite laminates with $0^o/90^o$ were made by T700/epoxy prepreg of thickness 0.15 mm (T700/epoxy composite, Beijing Institute of Aeronautical Materials, China), the properties of the unidirectional prepreg used in our experiments are provided in Table 1. Two pieces of honeycomb plates were cut by electronic engraving machine (Harbin Weijifen Organic Glass Products Co., Ltd.), and then these plates are assembled together basing on interlocking method. Each plate interlocked with other plate only from the long caulking groove in order to form egg lattice cores and each plate interlocked with other plates including both long and short caulking grooves to form pyramidal honeycomb cores. The fabricated egg and pyramidal honeycomb sandwich beams are sketched in Figure 8 (a) and (b), respectively. Finally, two face sheets will be bonded on the top and bottom of the honeycomb core to form a sandwich panel.

The relative density of egg honeycombs core can be approximated from

$$\bar{\rho} = \frac{d[(b+a-2t)(H-h)+2ah-d]}{a^2 H} \tag{7}$$

where the geometrical parameters, b, H, h, t, d and ω are shown in the schematic figure of the unit cell of the egg and pyramidal honeycomb structure shown in our previous paper. The relative density of pyramidal honeycomb cores is two times of that of egg honeycomb cores. In our samples, all the core relative densities have been calculated basing on analytical parameters of specimens, ranging from 3.0% to 6.0%. The pyramidal honeycomb structure shown in Fig. 2(a) has b = 12 mm, H = 20 mm, h = 8 mm, d = 2 mm. These sandwich structures were fabricated by attaching the pyramidal honeycomb structures to flat carbon fiber reinforced face sheets with adhesive (08-57, Heilongjiang Institute of Petrochemical).

2.2 Three point bending tests

In this section, we performed three point bending tests on sandwich panel specimens with different geometries. Prior to the bending experiments, the ends of the panels were first bonded to a U-shaped steel sheet (t_s =0.5 mm and length S =30 mm) and filled with an epoxy resin in order to prevent face sheet debonding as shown schematically in Figure 8. In this figure, L denotes the beam span and H and h_f are the core thickness and face sheet thickness, respectively. Both pyramidal and egg honeycomb structures with two different face sheet thicknesses were studied. In the experiments, the sandwich panel was supported by two 30 mm diameter hardened steel pins attached to a flat support base. The indenter had a flat central region 12.7 mm wide, with adjacent filets of 2 mm radius, and was moved at a constant rate of 0.02mm/s. The applied load was recorded by an INSTRON 5569 testing machine during the bending tests.

3. Theoretical Investigation of Bending Behavior

3.1 Analytical predictions of deflection and failure load

Allen [35] gives the total deflection δ at the mid-point of a sandwich beam loaded in three point bending as the sum of the deflections due to bending of the face sheets and shear of the honeycomb core:

$$\delta = \delta_B + \delta_S = \frac{PL^3}{48(EI)_{eq}} + \frac{PL}{4(AG)_{eq}} \tag{1}$$

Where $(EI)_{eq}$ is the equivalent flexural rigidity and $(AG)_{eq}$ is the equivalent shear rigidity

$$(AG)_{eq} = wHG_c \qquad (2)$$

Where G_c is the shear stiffness of the three-dimensional honeycomb core, which can be obtained from the shear experiment. For long beams with good shear stiffness, shear deformations are generally recognized as being negligible. However, when beams are short and/or have very poor shear properties, shear deformation could be significant or even dominant. In this paper, we will show how the low-density core leads to low "G_c" and, therefore, reduced three point bending stiffness and increased failure susceptibility.

Under three point bending, possible failure modes of a carbon fiber sandwich panel are: (i) face sheet crushing or wrinkling, (ii) core member crushing (including the honeycomb core's delamination or fracture) and (iii) debonding between the face sheet and honeycomb cores. The collapse of the panel is generally dictated by one of the competing mechanisms that depend on the geometry of the panel and the mechanical properties of the face and core materials. Fan et al [31] studied the three point bending behavior of carbon fiber composite sandwich panels with Kagome grid cores. Face buckling, debonding and core shear have been studied in three point bending experiments. However, the analytical estimates of the failure force for each mode were not studied well. Here, we adopted a similar method, which was used to derive the analytical models for failure initiation of carbon fiber composite sandwich beams with lattice cores presented in the papers [36], to obtain estimates of the failure load for the above modes of both egg and pyramidal honeycomb cores. In our analysis, we assumed that the core carries the shear load and the faces carry the applied moment; the cross-section method is shown in Figure 3 and 4 for egg and pyramidal honeycomb sandwich beams, respectively. The results are summarized below for the different failure modes mentioned above. Sandwich panel failure is dictated by the mode with the lowest value of applied load, P. We assumed that face sheet intra-cell buckling and core member buckling were not present in our experiments, with the analytical models thus given below:

(i) Face sheet crushing or wrinkling: The critical loads associated with each of the failure loads can be estimated from:

$$P_{FC} = \frac{4\sigma_{fy} h_f H w}{L} \quad \text{(face sheet crushing)} \quad (3)$$

$$P_{FW} = \frac{k_1 E_f \pi^2 h_f^3 (H + h_f) w}{3 l_1^2 L} \quad \text{(face sheet wrinkling)} \quad (4)$$

where σ_{fy} and E_f are the out-of-plane compressive crushing strength and compressive Young's modulus of the face sheets. The parameter k_1 depends on the end constraints during face sheet wrinkling. The mutual coupling effect between the core and face sheets was disregarded in the analytical models, and k_1 =1 was assumed in above equation to be a pinned connection. L is the span of the specimen under three point bending, l_1 is the wavelength between the point of two unit cells, where $l_1 = \frac{\sqrt{2}}{2}(a-b)$ and $a-b$ are for pyramidal and egg honeycomb cores, respectively.

(ii) Core member crushing: The pertinent failure loads associated with each failure load are:

$$P_{CC} = \frac{2\sigma_c dbw}{l_2} \quad \text{(core member crushing)} \quad (5)$$

where σ_c and E_c are the compressive strength and stiffness of the trapezoid plate of honeycomb cores. l_2 is the width of the unit cell and $l_2 = \frac{\sqrt{2}}{2}a$, $2a$ are for pyramidal and egg honeycombs cores, respectively.

(iii) Debonding between the face sheet and honeycomb core: The debonding between the three dimensional honeycomb core and face sheets was assumed to occur at a uniform shear strength τ_a, and additional strength is provided by the face sheets. The collapse load in three point bending with debonding failure can be expressed as:

$$P = 2wH\tau_{cr} \tag{6}$$

where τ_{cr} is the shear strength of the carbon fiber three-dimensional honeycomb structures, which can be obtained from the results presented in Section 2 and $\tau_{cr} = \tau_a A / l_2^2$.

3.2 Failure mechanism maps

In this section, we provide predictive failure maps for carbon fiber reinforced composite pyramidal and egg honeycomb sandwich panels based on analytical parameters. The approximate method is used to draw the failure mechanism map. Three different stacking sequences and two types of three-dimensional honeycomb cores have been considered in order to draw the failure mechanism map under three point bending, as listed in Table 2. Face wrinkling, Face crushing, core member crushing and core debonding are studied in our maps. As shown in Figure 5, 6 and 7, The stacking sequence and thickness of the face sheets can have a significant effect on the overall behavior and failure of composite sandwich panels.

3.3 Model validation

In three point bending tests, the total deformation of the specimens was calculated from equation (1) based on experimental parameters, and the percent of shear deformation and bending deformation was also calculated. Both are summarized in Table 3.

It was found that when the shear stiffness is invariant, the slope of load vs. displacement is larger and the percent of shear deformation in total deformation becomes larger as the face sheet becomes thicker. When the shear stiffness is changed to be smaller, shear deformation can be greater. In general, the test P/δ is in good agreement with the predictive value. The first reason for the deviation between the analytical calculation and the experiment is that the shear deflection was restricted by the end; the second reason is that the shear deformation of the face sheet was not considered in the analytical models. The adhesion strength between the three-dimensional honeycomb cores and face sheet appeared to be the limiting factor in several cases; debonding is always the last and dominant failure mode, as explained below. Almost all the beams failed by the predicted dominant mode, and some failure modes can occur at the same time due to the complex of the composite three-dimensional honeycomb cores, as summarized in Table 4. The strength of the three-dimensional honeycomb cores is much greater than that of the adhesive and the thin face sheet since there is no failure in the honeycomb core materials.

(i) Face sheet wrinkling: Face sheet wrinkling was predicted and observed in specimens 1 of both the pyramidal and egg honeycomb cores, which have a thin face sheet compared to specimen 2. The load displacement response and selected deformed configurations of specimen 1 of both pyramidal and egg honeycomb cores are shown in Figure 9. Prior to face wrinkling, the observed response is almost linear. The face wrinkling reduces the stability of the sandwich panels and induces debonding to occur between the face sheet and honeycomb cores; however, this does not result in a sudden drop in the load-carrying capacity of the specimen and thus is not a catastrophic event. As the deflection increased, the debonding between top face sheet and the three-dimensional honeycomb core led to a sudden drop of the load at ~ 1608.73 N. The calculated load by Equation (4) gives the force associated with the face wrinkling. The predicted load associated with the wrinkling is much lower than the peak failure load because wrinkling is not the dominant mode. The failure load predicted by Equation (6) for debonding between the face sheets and the honeycomb core is within 20% of the measured strength. This is probably due to the coupling between the pyramidal truss core and the face sheets, which was not considered in the analysis.

(ii) Debonding: Debonding is generally the dominant failure mode in the experiments for sandwich panels with three-dimensional honeycomb cores due to the higher shear strength of core materials compared to that of the adhesive. The representative load versus displacement and the failure modes are shown in Figure 10. For specimen 2, the top face sheet debonds from the core led to a sudden drop of the load while the bottom face sheet was still attached to the egg or pyramidal honeycomb core. After debonding, the residual loading capacity of specimen 8 was about 2000N, or 38% of the peak loading. The predicted debonding failure loads for all the specimens are somewhat lower than the measurements. This is probably due to the reinforcement of the two ends, which may have increased the peak load.

4. Computational Analysis

Linear-elastic analysis of the beam was conducted using finite element (FE) analysis. As noted earlier, the bending behavior of sandwich beams with three-dimensional honeycomb cores is very complex, and several simplifications have been made for the analytical models to predict the bending properties. The FE simulations were conducted in order to study the displacement of sandwich beams with three-dimensional honeycomb cores accurately under the same applied bending load, 1500 N. The adhesive strength between the honeycomb core and the face sheet was assumed to be sufficiently strong to transmit the load between the core and face sheet.

The sandwich beams with three-dimensional honeycomb cores were made with T700/3234 composite materials and were meshed using ABAQUS software with a fully integrated tetrahedron element with an ideal elastic model. The homogeneous material properties are listed in Table 2. Surface-to-surface contact was used to model the contact between the core and face sheet, as well as between the indenter and the top face sheet. These FE models were used to simulate these structures in order to determine the dependence of bending behavior on the span length, face thickness and core wall thickness. The bending behaviors of egg and pyramidal honeycomb sandwich beams calculated by the FE method are shown in Figure 11 (a) and (b), respectively. Comparisons of both three-dimensional honeycomb cores with different geometries were also carried out based on the simulation model. The effect between span length and the ratio of max displacement/applied load are shown in Figure 12. It is assumed that h_f=2 mm and d=2mm for both egg and pyramidal honeycomb cores. The ratio increases with increasing span length, and the range between the egg and pyramidal honeycomb cores becomes wider with this increment. This is due to the increasing maximum displacement of the sandwich beams—the span length is greater, and the contribution of the honeycomb core becomes smaller as the span increases. Figure 13 shows the relationship between the ratio of maximum displacement/failure load and the thickness of the face sheet. In this figure, the thickness of the core wall is the same for both honeycomb cores; d=2 mm. L=227.5 mm and 225.26 mm are the span length for the egg and pyramidal honeycomb beams, respectively.

It was discovered that the range between two curves becomes shorter with the increase of the face sheet thickness due to the contribution of the face sheet in the overall behavior. The relationship between the ratio of maximum displacement/failure load and the core wall thickness is shown in Figure 14. In this figure, the thickness of the face sheet is the same for both honeycomb cores, with h_f=2 mm. L=227.5 mm and 225.26 mm for the egg and pyramidal honeycomb cores, respectively. The ratio's value will decrease as the thickness of core wall increases; however, the range between the two curves will be narrower since the contribution made by the maximum displacement is dominated by the span length, and the ratio of the core wall's contribution is very limited. It can be concluded that the bending properties of pyramidal honeycomb sandwich beams are much superior to those of the egg honeycomb sandwich beams.

5. Conclusions

Carbon fiber composite sandwich panels with egg and pyramidal honeycomb cores have been designed and manufactured using the interlocking method. Three point bending tests were carried out to study the mechanical behaviors of the carbon fiber composite sandwich beams with egg and pyramidal honeycomb cores. Analytical models and failure maps were created in order to predict the mechanical response and failure modes of all the specimens with different face sheet thicknesses. Displacement at the center point was tested, and the analytical prediction for this was made by considering the contribution made by the face sheet and core materials in terms of bending and shear. Face wrinkling and debonding have been indicated under three point bending. In general, the measured displacement and peak loads obtained in the experiments were in good agreement with the analytical predictions. The bending data is very useful for designing sandwich beams with lightweight and multifunctional applications.

Acknowledgements

The present work was supported in part by the Major State Basic Research Development Program of China (973 Program) under grant No. 2011CB610303, National Science Foundation of China under grant Nos. 11222216, 11002041 and 11302060. JX also gratefully acknowledges Supported by Natural Scientific Research Innovation Foundation in Harbin Institute of Technology (HIT.NSRIF.2014025) and the National Key Lab of Materials and Structures in Special Environment.

References

[1] Qin QH, Wang TJ. Low-velocity impact response of fully clamped metal foam core sandwich beam incorporating local denting effect. Composite Structures 2013; 98: 346-356.

[2] Wang ZJ, Qin QH, Zhang JX, Wang TJ. Low velocity impact response of geometrically asymmetric slender sandwich beams with metal foam core. Composite Structures, 2013; 98: 1-14.

[3] Lu TJ, Liu T, Deng ZC. Thermoelastic properties of sandwich materials with pin-reinforced foam cores. Science in China Series E- Technological Sciences 2008; 51(22): 2059-2074.

[4] Zhang JX, Qin QH, Wang TJ. Compressive strength and dynamic response of corrugated metal sandwich plates with unfilled and foam-filled sinusoidal plate cores. Acta Mechanica 2013; 224(4): 759-775.

[5] Pan SD, Wu LZ, Sun YG, Zhou ZG. Fracture test for double cantilever beam of honeycomb sandwich panels. Materials Letters 2008; 62: 523-526.

[6] Hou SJ, Ren LL, Dong D, Han X. Crashworthiness optimization design of honeycomb sandwich panel based on factor screening. Journal of Sandwich Structures and Materials 2012; 14(6): 655-678.

[7] Lu TJ, Zhang QC. Novel strengthing methods for ultralightweight sandwich structures with periodic lattice cores. Science in China-Technological Sciences 2010; 53(3): 875-877.

[8] Zhang QC, Han YJ, Chen CQ, Lu TJ. Ultralight X-type lattice sandwich structure (I): Concept, fabrication and experimental characterization. Science in China Series E-Technological Sciences 2009; 52(8): 2147-2154.

[9]Ashby MF. Materials selection in mechanical design (Fourth edition). Boston: A Butterworth-Heinemann, 2010

[10] Petrone G, Rao S, De Rosa S, Mace BR, Franco F, Bhattacharyya D. Behaviour of fibre-reinforced honeycomb core under low velocity impact loading. Compos Struct 2013; 100: 356-362.

[11] Petrone G, Rao S, De Rosa S, Mace BR, Franco F, Bhattacharyya D. Initial experimental investigations on natural fibre reinforced honeycomb core panels. Compo Part B 2013; 55: 400-406.

[12] Han DY, Tsai SW. Interlocked composite grids design and manufacturing. J. Compos Mater 2003; 37: 287-316.

[13] Liu JY, Zhou ZG, Wu LZ, Ma L. A study on mechanical behavior of the carbon fiber composite sandwich panel with pyramidal truss cores at different temperatures. Science China: Physics, Mechanics and Astronomy 2012; 55(11): 2135-2142.

[14] Xiong J, Ma L, Vaziri A, Yang JS, Wu LZ. Mechanical behavior of carbon fiber composite lattice core sandwich panels fabricated by laser cutting. Acta Mater 2012; 60: 5322-5334.

[15] Ebrahimi H, Vaziri A. Metallic sandwich panels subjected to multiple intense shocks. International Journal of Solids and Structures 2013; 50: 1164-1176.

[16] Vaziri A, Hutchinson JW. Metallic sandwich plates subject to intense air shocks. Int J Solids Struct 2007; 44(1): 2021–2035.

[17] Xin FX, Lu TJ. Analytical modeling of fluid loaded orthogonally rib-stiffened sandwich structures: Sound transmission. Journal of the Mechanics and Physics of Solids 2010; 58: 1374-1396.

[18] Xin FX, Lu TJ. Sound radiation of orthogonally rib-stiffened sandwich structures with cavity absorption. Composites Science and Technology 2010; 70: 2198-2206.

[19] Kim T, Zhao CY, Lu TJ, Hodson HP. Convective heat dissipation with lattice frame materials. Mech Mater 2004; 36: 767-780.

[20] Liu J, Cheng YS, Li RF, Au FTK. A semi-analytical method for bending, buckling, and free vibration analyses of sandwich panels with square-honeycomb cores. Int J Struct Stab Dyn 2010; 10: 127-151.

[21] He L, Cheng YS, Liu J. Precise bending stress analysis of corugated-core, honeycomb core and X-core sandwich panels. Composite Structures 2012; 94: 1656-1668.

[22] Rathbun HJ, Wei Z, He MY, Zok FW, Evans AG, Sypeck DJ, Wadley HNG. Measurement and simulation of the performance of a lightweight metallic sandwich structure with a tetrahedral truss core. J Appl Mech 2004; 71: 368-374.

[23] Zok FW, Waltner SA, Wei Z, Rathbun HJ, McMeeking RM, Evans AG. A protocol for characterizing the structural performance of metallic sandwich panels: application to pyramidal truss cores. Int J Solids Struct 2004; 41(22-23): 6249-6271.

[24] Valdevit L, Hutchinson JW, Evans AG. Structurally optimized sandwich panels with prismatic cores. Int J Solids Struct 2004; 41(18-19): 5105-5124.

[25] Jin FN, Chen HL, Zhao L, Fan HL, Cai CG, Kuang N. Failure mechanisms of sandwich composites with orthotropic integrated woven corrugated cores: Experiments. Compos Struct 2013; 98: 53-58.

[26] Liu T, Deng ZC, Lu TJ. Analytical modeling and finite element simulation of the plastic collapse of sandwich beams with pin-reinforced foam cores. Int J Solids Struct 2008; 45(18-19): 5127-5151.

[27] Liu T, Deng ZC, Lu TJ. Design optimization of truss-cored sandwiches with homogenization. Int J Solids Struct 2006; 43(25-26): 7891-7918.

[28]Russell BP, Deshpande VS, Wadley HNG. Quasistatic deformation and failure modes of composite square honeycomb. J Mech Mater Struct 2008; 3:1315–1340.

[29] Russell BP, Liu T, Fleck NA, Deshpande VS. Quasi-static three-point bending of

carbon fiber sandwich beams with square honeycomb cores. J Appl Mech 2011; 78: 031008-1-031008-15.

[30] Li M, Wu LZ, Ma L, Wang B, Guan ZX. Structural design of pyramidal truss core sandwich beams loaded in 3-point bending. J Mech Mater Struct 2011; 6: 1255-1266

[31] Fan HL, Meng FH, Yang W. Sandwich panels with Kagome lattice cores reinforced by carbon fibers. Compos Struct 2007; 81: 533-539.

[32] Fan HL, Yang L, Sun FF, Fang DN. Compression and bending performances of carbon fiber reinforced lattice-core sandwich composites. Compos part A 2013; 52: 118-125.

[33] Xiong J, Hu H, Zhang M, Zhang Z, Ma L, Wu LZ. Compression behavior and energy absorption of carbon fiber reinforced composite sandwich panels made of three -dimensional grid cores. submitted.

[34] Xiong J, Zhang M, Stocchi A, Hu H, Ma L, Wu LZ, Zhang Z. Mechanical behaviors of carbon fiber composite sandwich columns with three dimensional honeycomb cores under in-plane compression. Submitted.

[35] Allen HG. Analysis and design of structural sandwich panels. New York: Pergamon Press, 1969.

[36] Xiong J, Ma L, Pan SD, Wu LZ, Papadopoulos J, Vaziri A. Shear and bending performance of carbon fiber composite sandwich panels with pyramidal truss cores. Acta Mater 2012; 60: 1455-1466.

Figures

Fig.1 Photographs of (a) pyramidal honeycomb cores and (b) sandwich panels with $\bar{\rho} = 6.0\%$

Fig.2 Photographs of (a) egg honeycomb cores and (b) sandwich panels with $\bar{\rho} = 3.0\%$

Fig. 3. Force analysis model of sandwich beams with egg honeycomb cores (a) under three point bending, (b) top view, (c) section method for egg honeycomb cores under three point bending, (d) typical unit cell of egg honeycomb cores bearing shear load *V* (absent the top face sheet). The decomposition of force for sandwich panels with egg honeycomb cores under three point bending are similar with above section method.

Fig. 4. Force analysis model of sandwich panels with pyramidal honeycomb cores (a) under three point bending, (b) top view, (c) section method for pyramidal honeycomb cores under three point bending, (d) typical unit cell of pyramidal honeycomb cores bearing shear load *V* (absent the top face sheet). The decomposition of force for sandwich panels with pyramidal honeycomb cores under three point bending are similar with above section method.

Fig. 5. Failure mechanism maps for carbon fiber composite sandwich beams with egg and pyramidal honeycomb cores under three point bending. Face sheets with $[0^o/0^o/0^o/0^o]_n$ were considered in both maps.

Fig.6. Failure mechanism maps for carbon fiber composite sandwich beams with egg and pyramidal honeycomb cores under three point bending: FW = face sheet wrinkling; FC = face sheet crushing; CC = core member crushing; CD = core debonding. Face sheets with $[0^o/90^o/90^o/0^o]_n$ were considered and both mechanism maps were used to design the specimens.

Fig. 7. Failure mechanism maps for carbon fiber composite sandwich beams with egg

and pyramidal honeycomb cores under three point bending. Face sheets with [90 ^{o} /90 ^{o} /90 ^{o} /90^{o}]$_{n}$ were considered for drawing above mechanism maps.

Fig.8 Fabrication of sandwich beams with 3D honeycomb cores for three point bending tests by using cut carbon fiber reinforced composite sheets and interlock method: (a) Egg honeycomb cores; (b) Pyramidal honeycomb cores.

Fig. 9. (a) Bending response and deformed configurations of egg-specimen 1 and pyramidal-specimen 1. (b) and (c) are the failure modes of egg and pyramidal honeycomb cores, respectively. Both face wrinkling and debonding modes were observed during the bending experiments. The sudden drop in the panel peak strength is mainly due to the core debonding.

Fig. 10. (a) Bending response and deformed configurations of egg-specimen 2 and pyramidal-specimen 2. Debonding modes were observed during the bending experiments for (b) egg honeycomb cores and (c) pyramidal honeycomb cores.

Fig.11 Bending behaviors for (a) Egg and (b) pyramidal honeycomb sandwich beams done by simulation.

Fig. 12 The relationship between the ratio (Max displacement / Applied load) of 3D honeycomb sandwich beams and span length

Fig. 13 The relationship between the ratio (Max displacement / Applied load) of 3D honeycomb sandwich beams and thickness of face sheet, h_f

Fig. 14 The relationship between the ratio (Max displacement / Applied load) of 3D honeycomb sandwich beams and the thickness of core wall, d

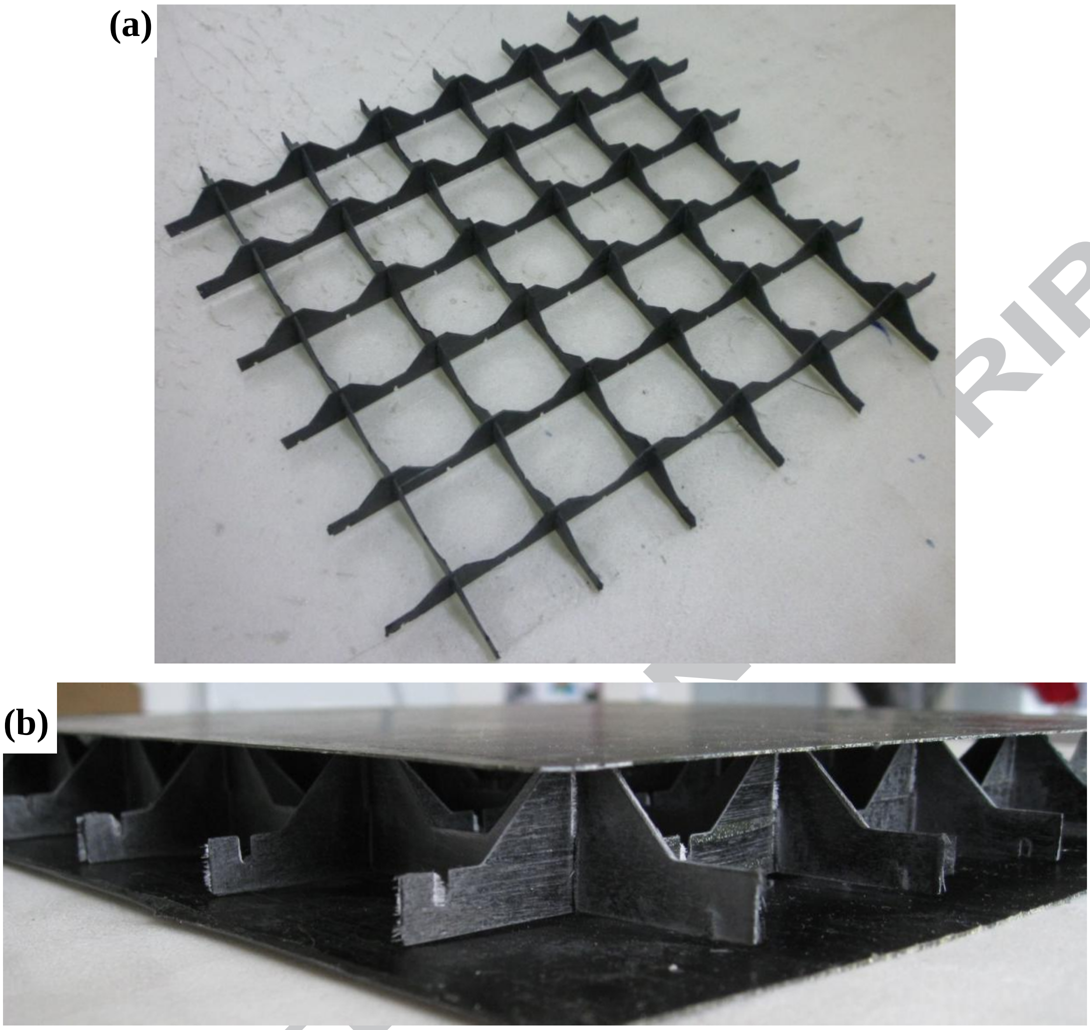

Fig.1 Photographs of (a) egg honeycomb cores and (b) sandwich panels with $\bar{\rho} = 3.0\%$

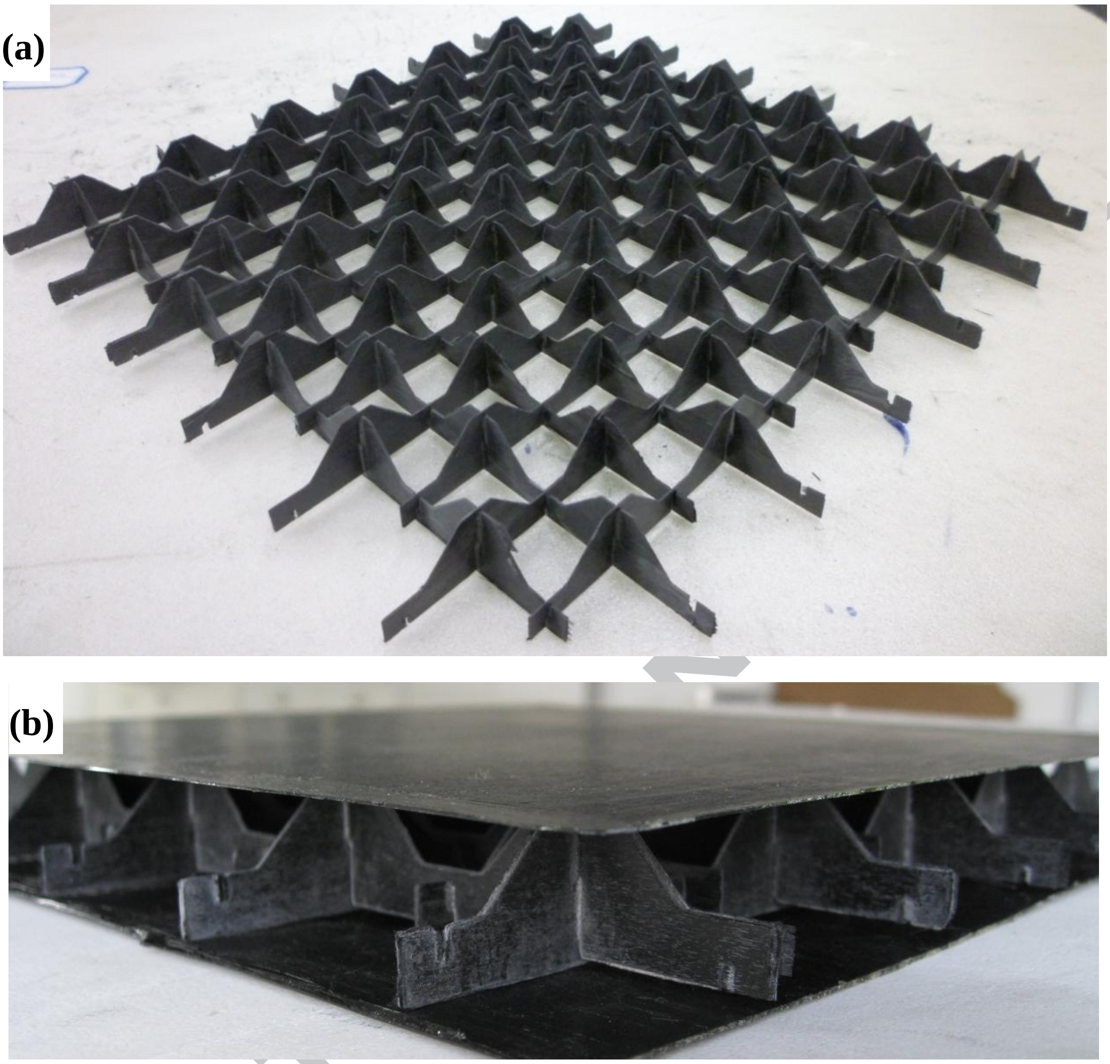

Fig.2 Photographs of (a) pyramidal honeycomb cores and (b) sandwich panels with $\bar{\rho} = 6.0\%$

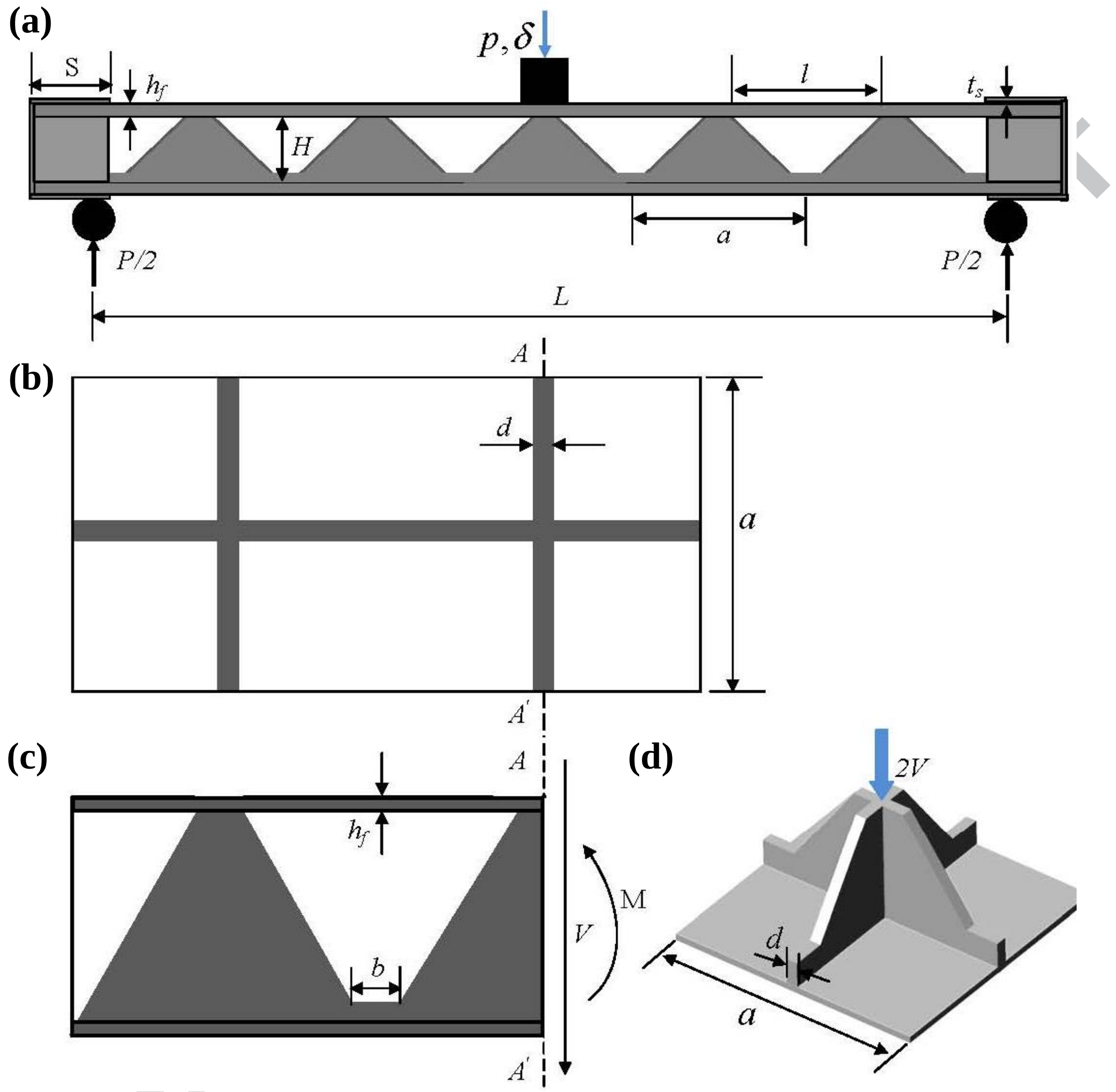

Fig. 3. Force analysis model of sandwich beams with egg honeycomb cores (a) under three point bending, (b) top view, (c) section method for egg honeycomb cores under three point bending, (d) typical unit cell of egg honeycomb cores bearing shear load *V* (absent the top face sheet). The decomposition of force for sandwich panels with egg honeycomb cores under three point bending are similar with above section method.

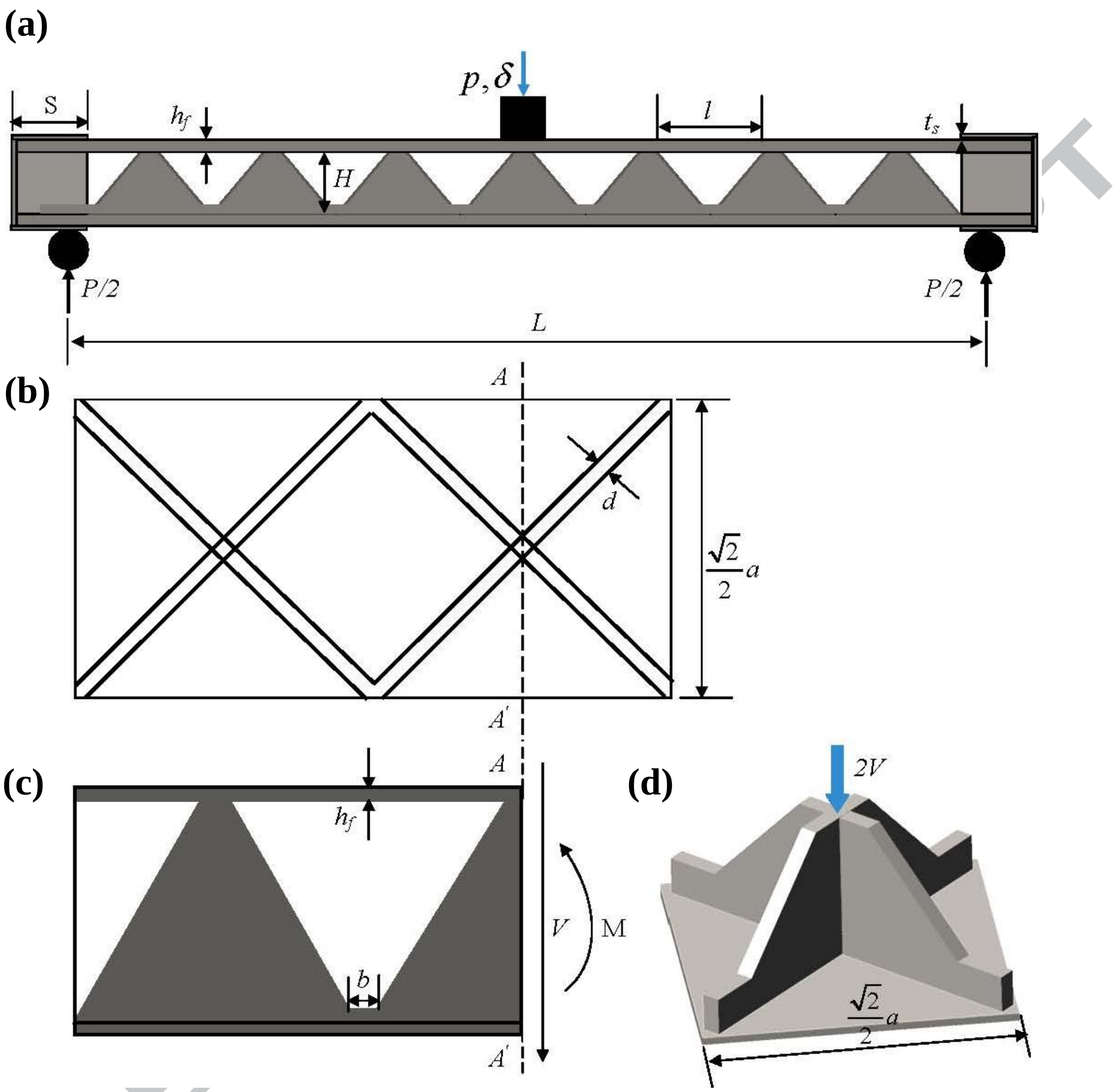

Fig. 4. Force analysis model of sandwich panels with pyramidal honeycomb cores (a) under three point bending, (b) top view, (c) section method for pyramidal honeycomb cores under three point bending, (d) typical unit cell of pyramidal honeycomb cores bearing shear load V (absent the top face sheet). The decomposition of force for sandwich panels with pyramidal honeycomb cores under three point bending are similar with above section method.

(a)

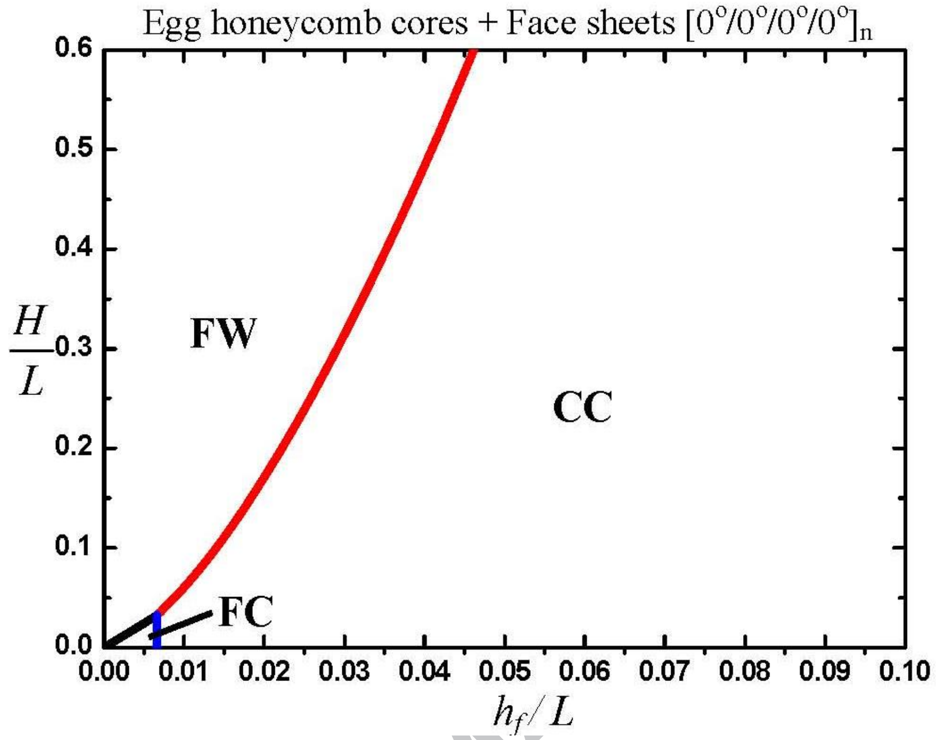

(b)

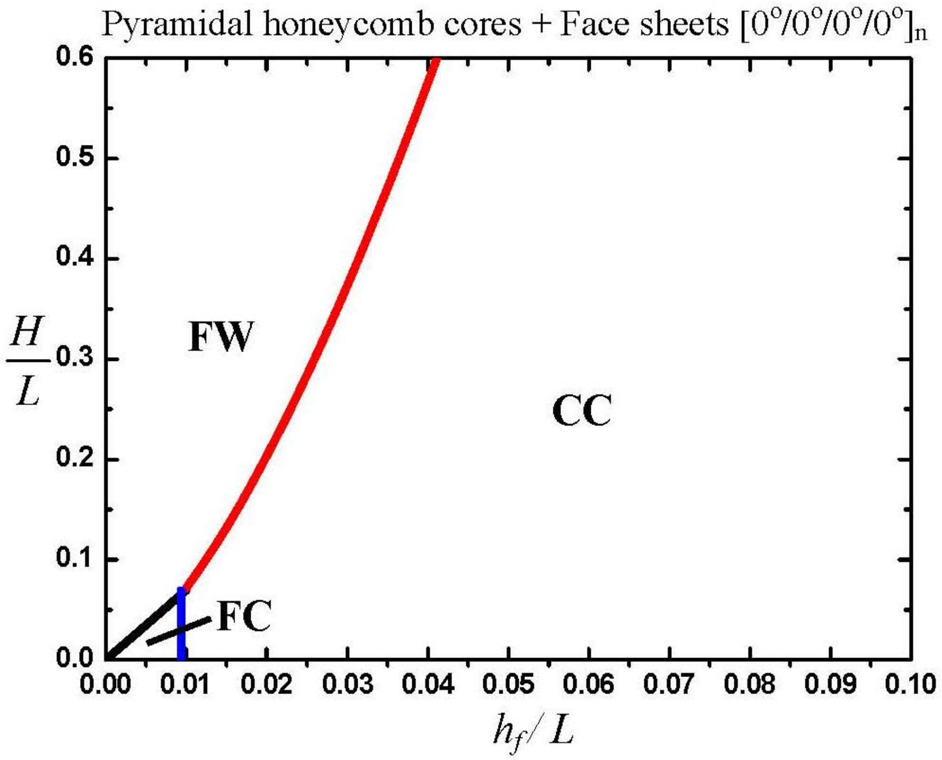

Fig. 5. Failure mechanism maps for carbon fiber composite sandwich beams with egg and pyramidal honeycomb cores under three point bending. Face sheets with $[0^{o}/0^{o}/0^{o}/0^{o}]_n$ were considered in both maps.

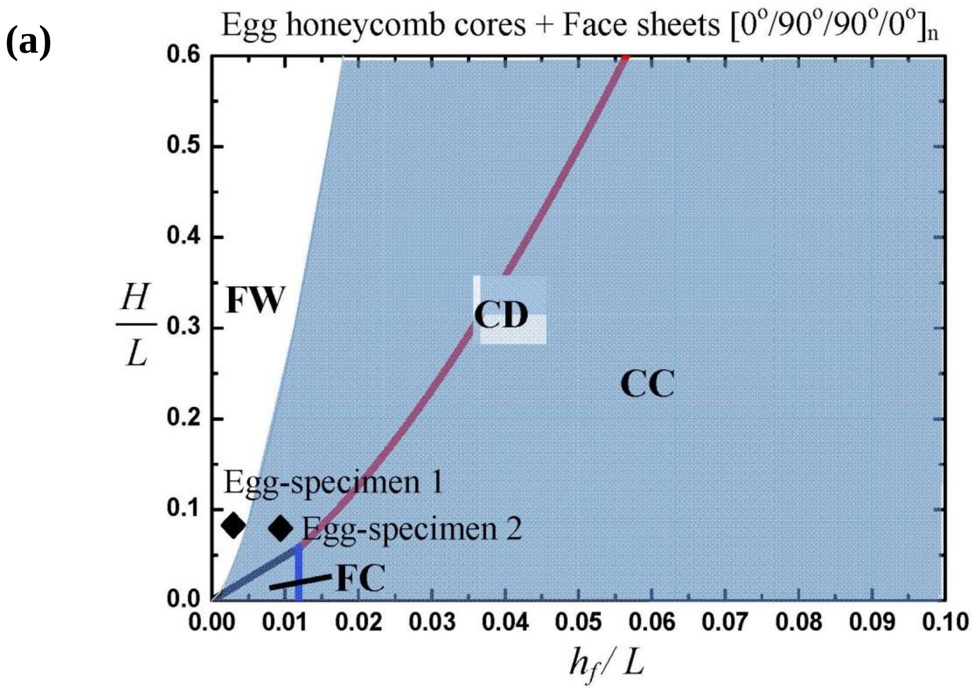

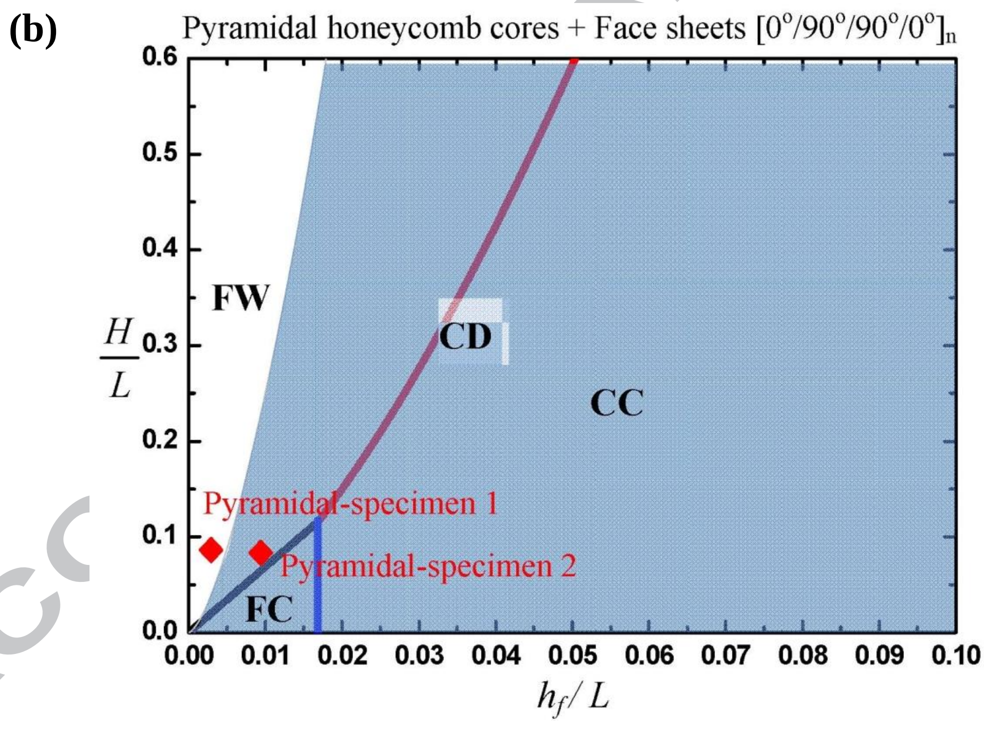

Fig.6. Failure mechanism maps for carbon fiber composite sandwich beams with egg and pyramidal honeycomb cores under three point bending: FW = face sheet wrinkling; FC = face sheet crushing; CC = core member crushing; CD = core debonding. Face sheets with $[0^{o}/90^{o}/90^{o}/0^{o}]_n$ were considered and both mechanism maps were used to design the specimens.

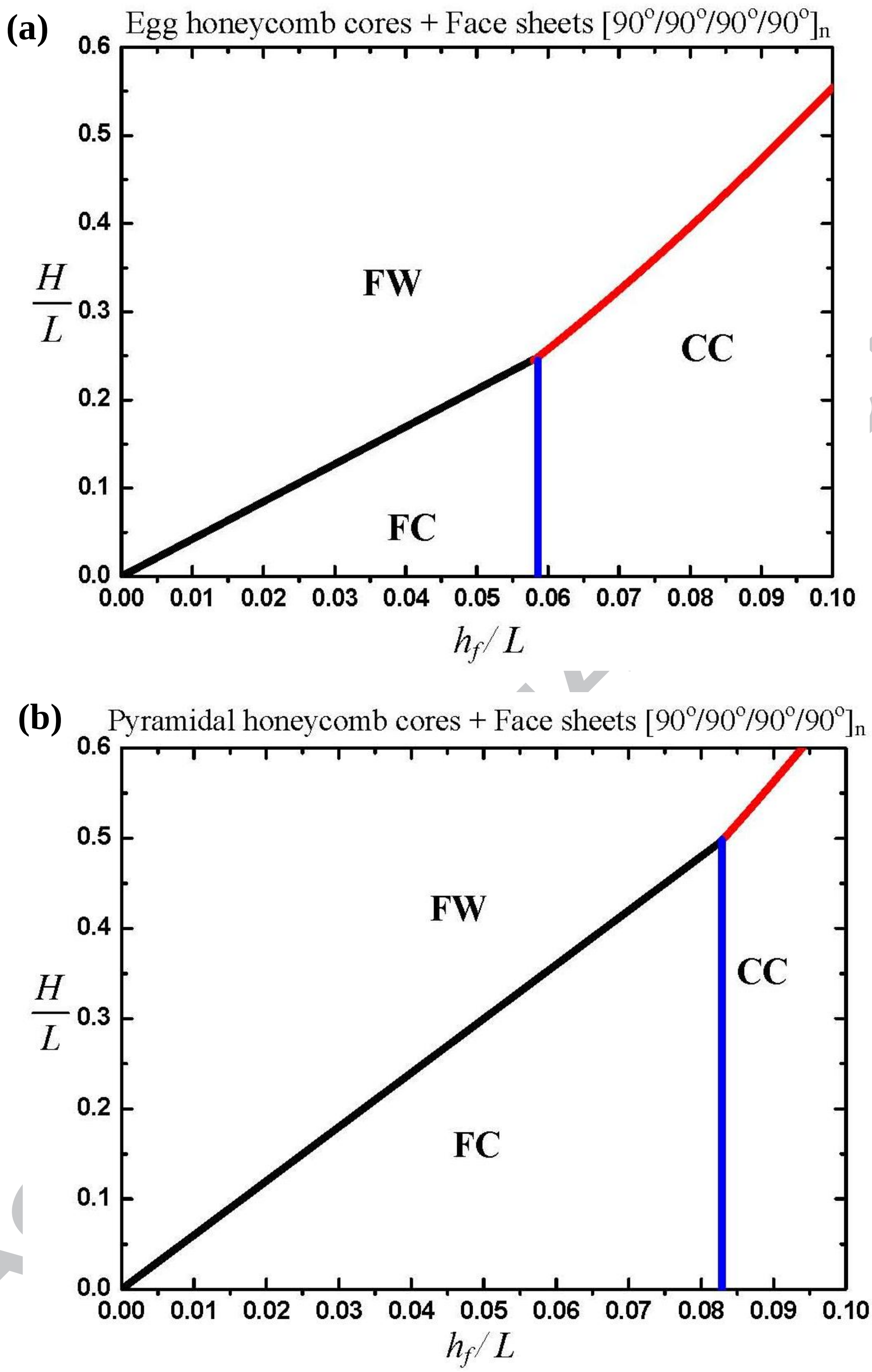

Fig. 7. Failure mechanism maps for carbon fiber composite sandwich beams with egg and pyramidal honeycomb cores under three point bending. Face sheets with [90 ^{o} /90 ^{o} /90 ^{o} /90^{o}]$_{n}$ were considered for drawing above mechanism maps.

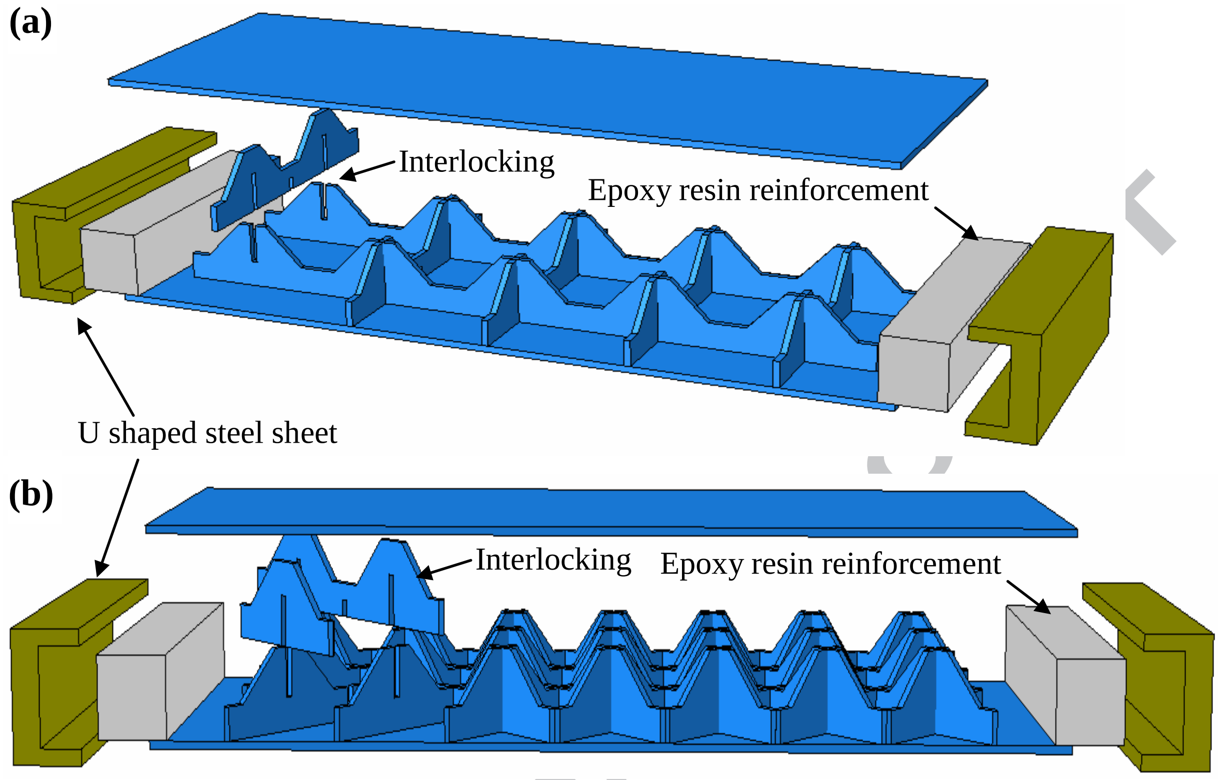

Fig.8 Fabrication of sandwich beams with 3D honeycomb cores for three point bending tests by using cut carbon fiber reinforced composite sheets and interlock method: (a) Egg honeycomb cores; (b) Pyramidal honeycomb cores.

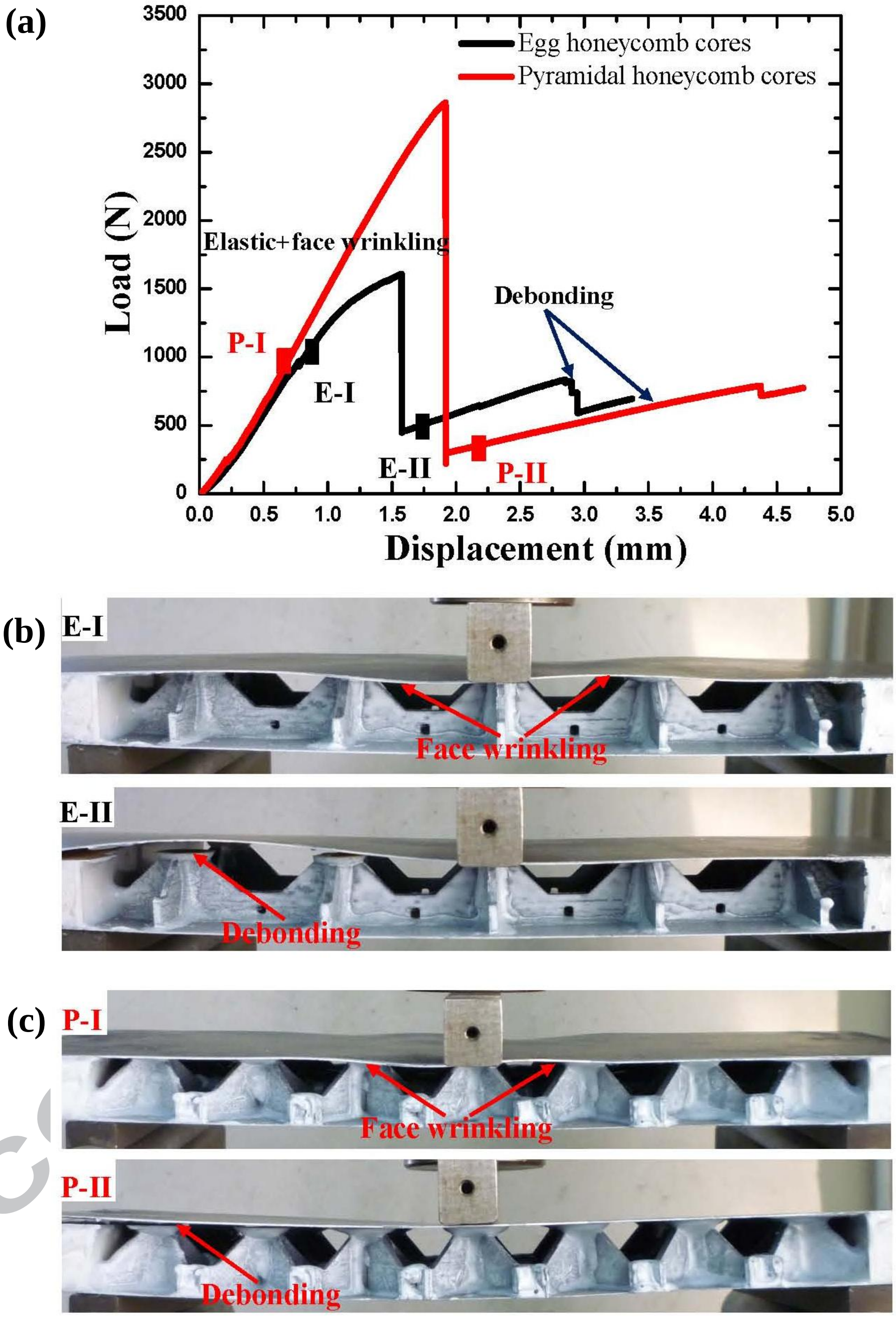

Fig. 9. (a) Bending response and deformed configurations of egg-specimen 1 and pyramidal-specimen 1. (b) and (c) are the failure modes of egg and pyramidal honeycomb cores, respectively. Both face wrinkling and debonding modes were observed during the bending experiments. The sudden drop in the panel peak strength is mainly due to the core debonding.

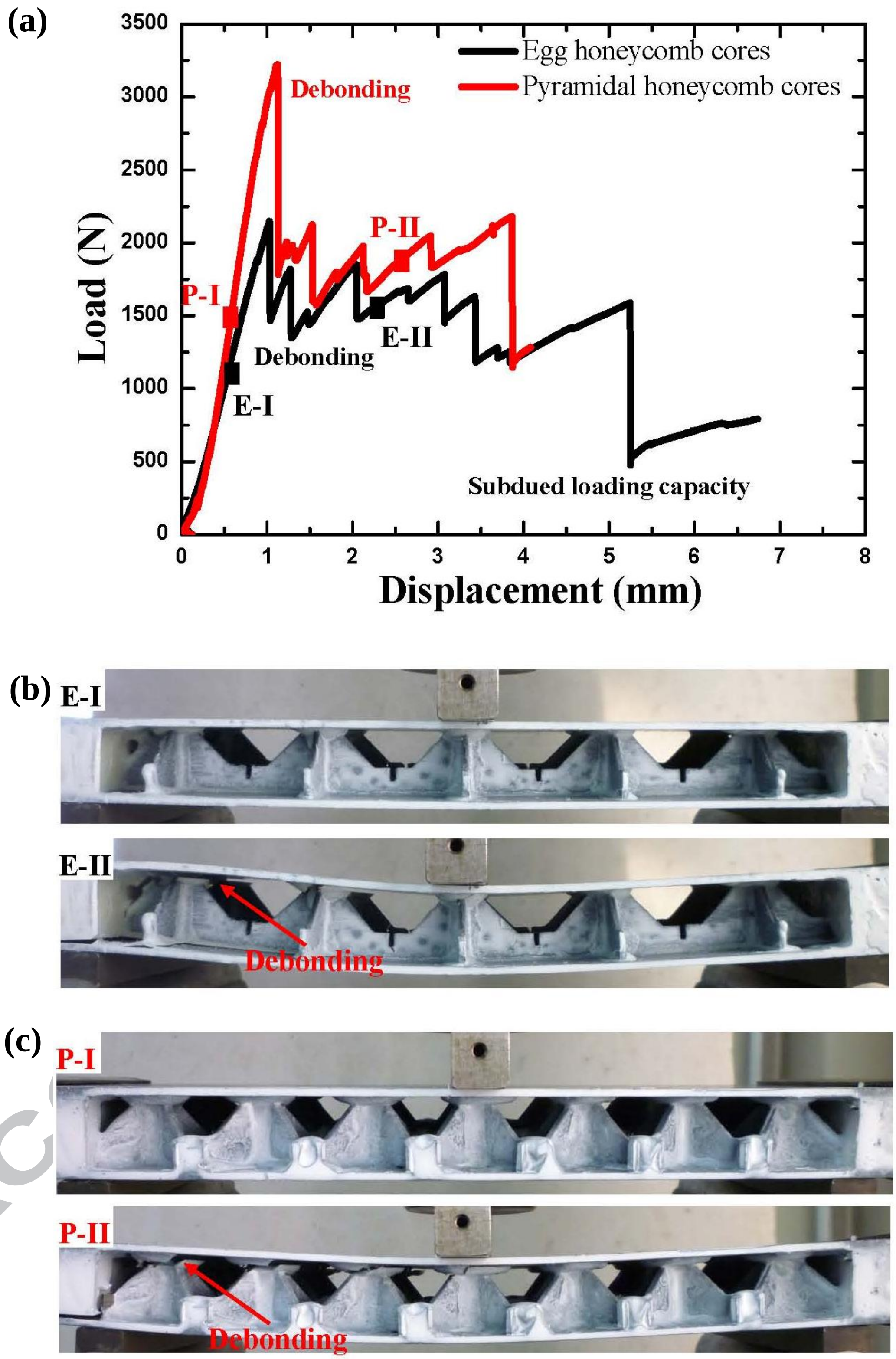

Fig. 10. (a) Bending response and deformed configurations of egg-specimen 2 and pyramidal-specimen 2. Debonding modes were observed during the bending experiments for (b) egg honeycomb cores and (c) pyramidal honeycomb cores.

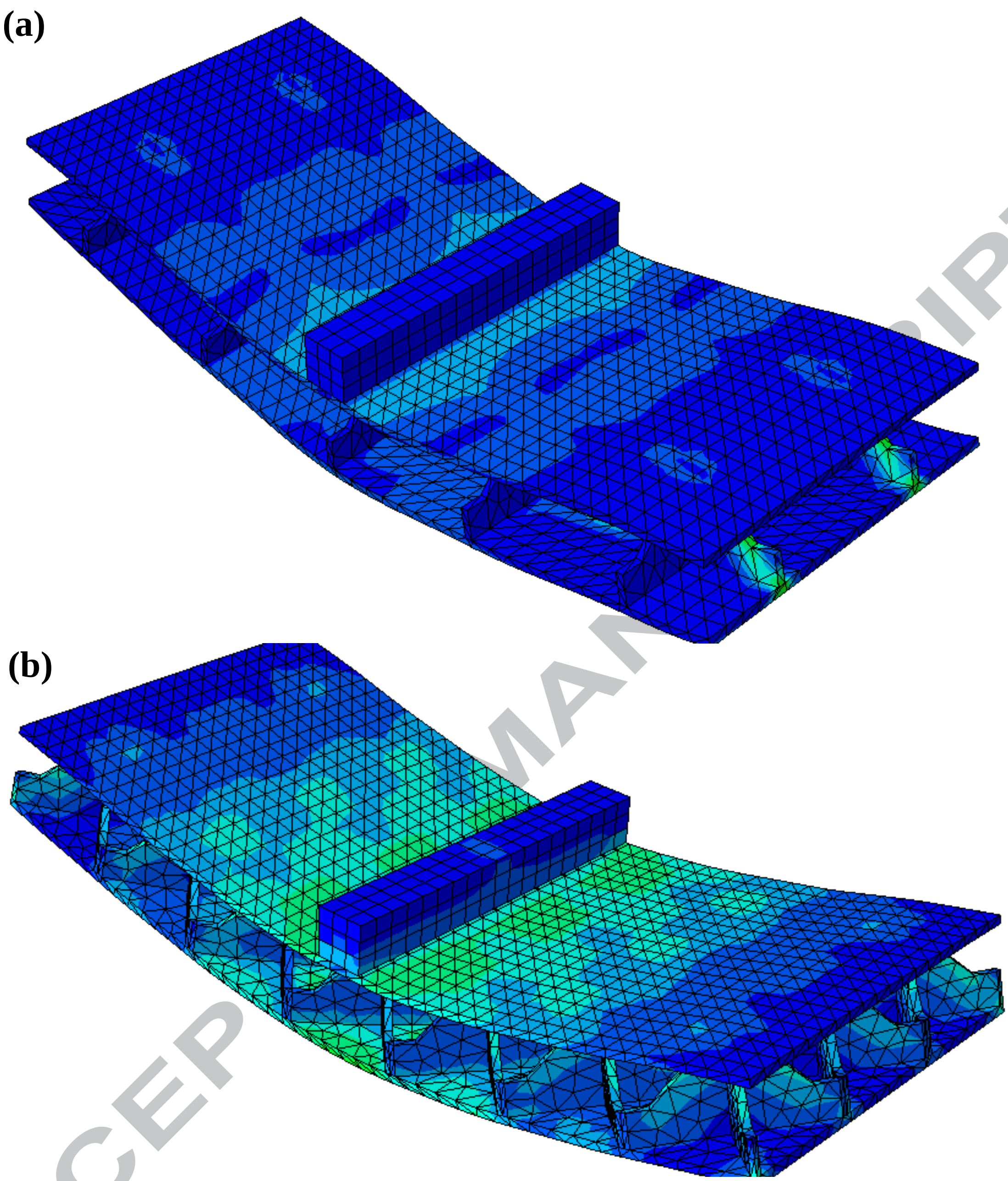

Fig.11 Bending behaviors for (a) Egg and (b) pyramidal honeycomb sandwich beams done by simulation.

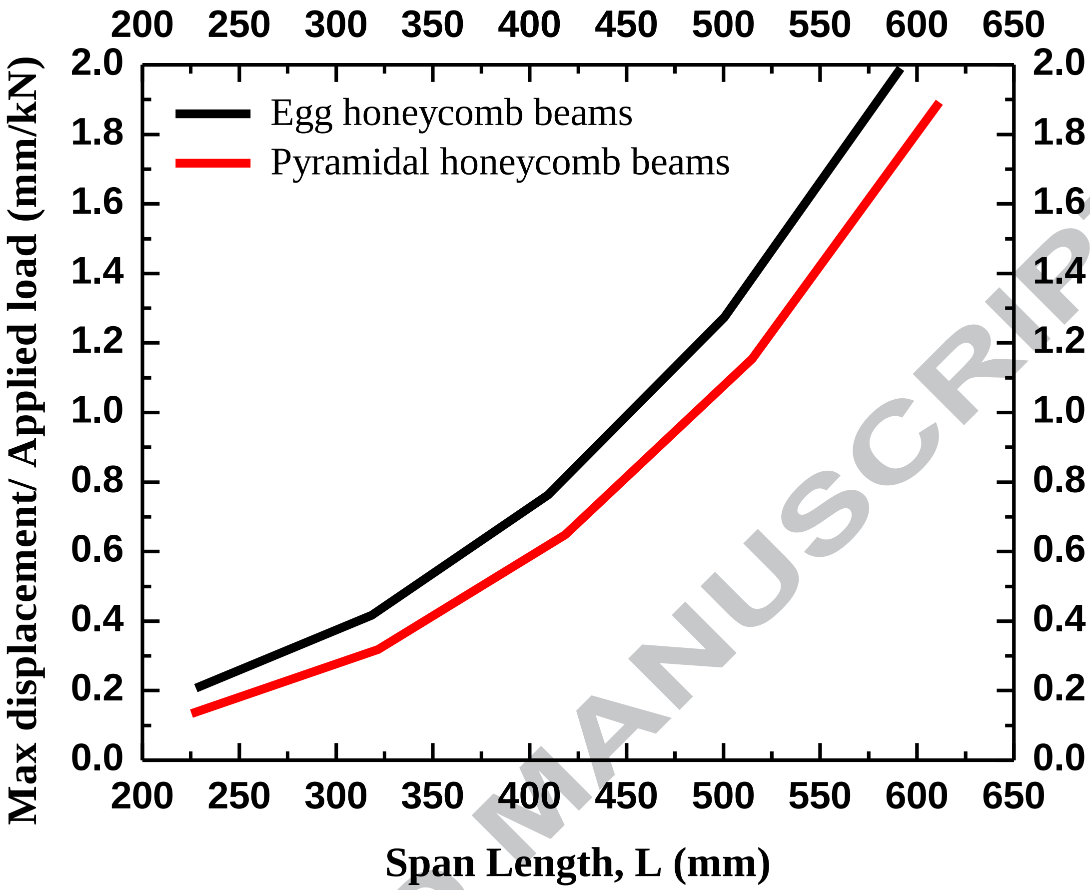

Fig. 12 The relationship between the ratio (Max displacement / Applied load) of 3D honeycomb sandwich beams and span length

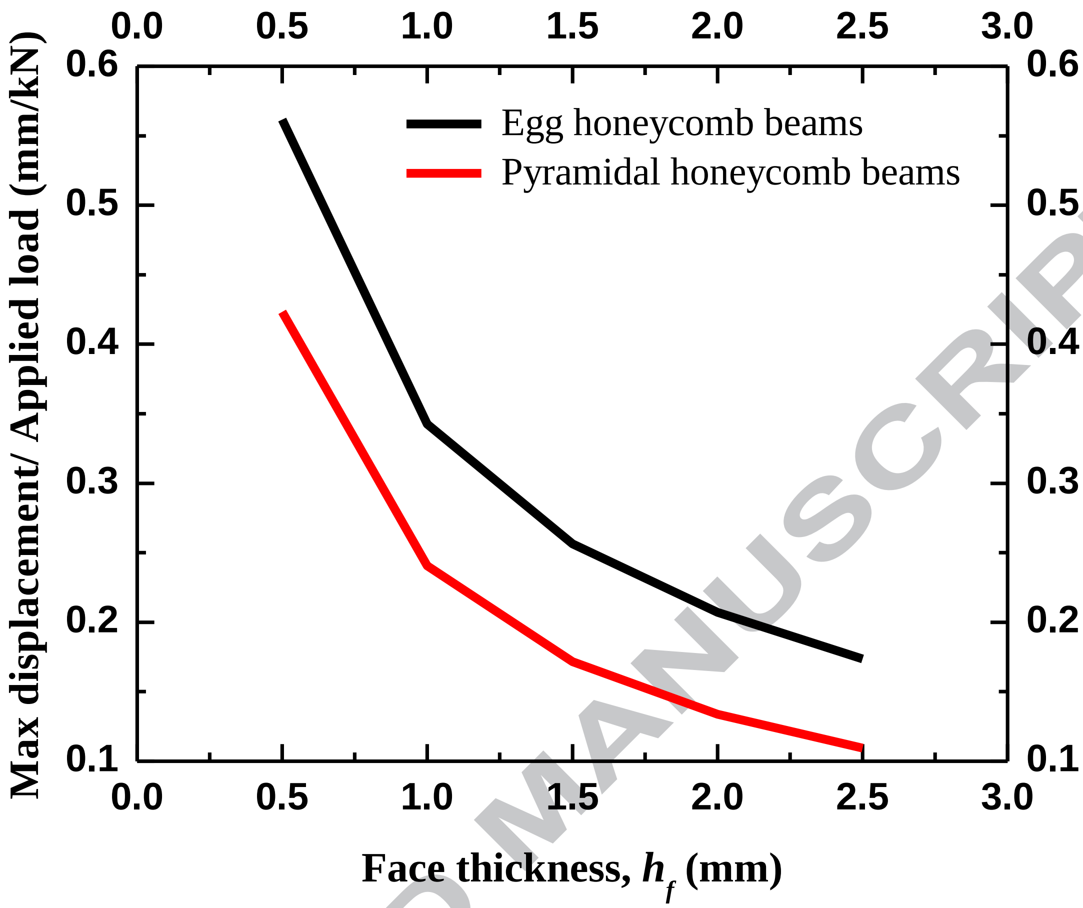

Fig. 13 The relationship between the ratio (Max displacement / Applied load) of 3D honeycomb sandwich beams and thickness of face sheet, h_f

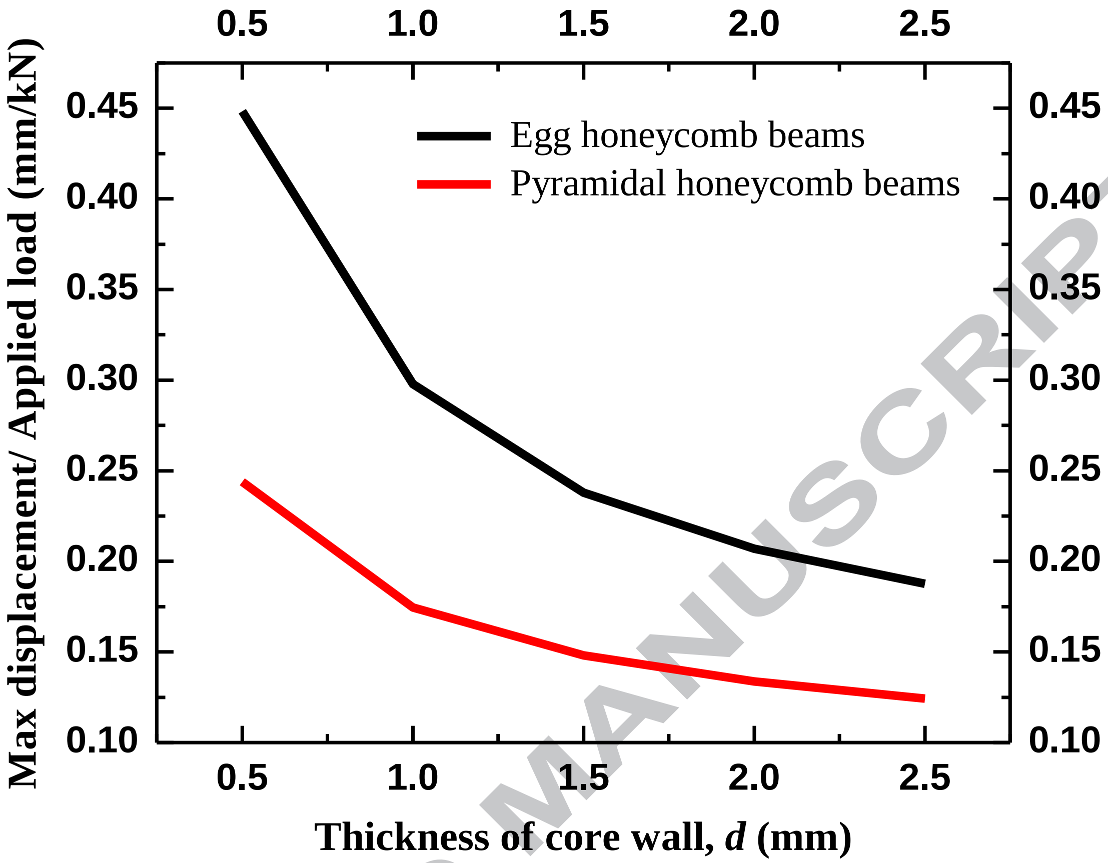

Fig. 14 The relationship between the ratio (Max displacement / Applied load) of 3D honeycomb sandwich beams and the thickness of core wall, *d*

Tables

Table 1 Properties of unidirectional lamella (*T700/epoxy composites*).

Table 2 Mechanical properties of carbon fiber composite face-sheets and slender laminate sheets of honeycomb cores

Table 3 Three point bending deformation of 3D honeycomb cores along with predicted and measured P/δ (N/mm) and the center deflection δ (mm)

Table 4 Summary of the geometries employed in three point bending tests along with the predicted and measured failure loads and collapse modes

Table 1

Properties of unidirectional lamella (*T700/epoxy composites*).

Properties	Value
0°Tensile strength (MPa)	1400
0°Tensile modulus (GPa)	123
90°Tensile strength (MPa)	18
90°Tensile modulus (GPa)	8.3
0°Compression strength (MPa)	850
0°Compression modulus (GPa)	100
90°Compression strength (MPa)	96
90°Compression modulus (GPa)	8.4
In-plane shear strength (MPa)	16.0
In-plane shear modulus (GPa)	4.8

Interlayer shear strength (Mpa)	60
Poisson's ratio	0.3
Volume fraction of fibers	57%±3
Density(kg/m^3)	1550

Table 2 Mechanical properties of carbon fiber composite face-sheets and slender laminate sheets of honeycomb cores

No.	Stack sequence	E_f (GPa)	σ_{fy} (MPa)	E_c (GPa)	σ_c (MPa)
a)	$(0°/0°/0°/0°)_s$	100	850	54.504	473
b)	$(0°/90°/90°/0°)_s$	54.504	473	54.504	473
c)	$(90°/90°/90°/90°)_s$	8.4	96	54.504	473

Table 3 Three point bending deformation of 3D honeycomb cores along with predicted and measured P/δ (N/mm) and the center deflection δ (mm)

Specimen		δ_B and δ_S (mm)	Analy. total δ (mm)	Analy. P/δ (N/mm)	Percent (%)	Test P/δ (N/mm)	Test δ(mm)	Fail. load P (N)
Egg honeycomb cores	1	0.73 0.45	1.18	1360.24	61.97 38.03	1491.53	1.57	1608.73
	2	0.26 0.60	0.86	2507.37	29.79 70.21	2547.31	1.03	2146.70
Pyramidal honeycomb cores	1	1.15 0.45	1.60	1787.72	72.03 27.97	1802.71	1.92	2862.77
	2	0.35 0.50	0.85	3774.29	40.99 59.01	3981.14	1.12	3222.87

Table 4 Summary of the geometries employed in three point bending tests along with the predicted and measured failure loads and collapse modes

Topologies	No	w (mm)	L (mm)	h_f (mm)	Analy. Fail Mode	Analy. Fail force (N)	Obs. Fail mode	Obs. Fail force (N)
Egg honeycomb cores	1	90.21	223.6	0.52	FW	322.2	FW & CD	1608.73
					FC	7937.8		
					CC	35665.6		
					CD	1292.8		
	2	90.07	225.6	2.05	FW	20994.9	CD	2146.70
					FC	30973.1		
					CC	35610.3		
					CD	1290.8		
Pyramidal honeycomb cores	1	92.86	220.8	0.55	FW	398.0	FW & CD	2862.77
					FC	8751.9		
					CC	36713.3		
					CD	2661.7		
	2	93.39	221.9	2.06	FW	22461.3	CD	3222.87
					FC	32800.7		
					CC	36922.9		
					CD	2676.8		